

Temperature-modulated electronic structure of graphene on SiC: Possible roles of electron-electron interaction and strain

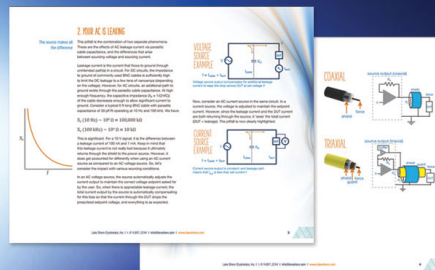
Choongyu Hwang, Jinwoong Hwang, Ji-Eun Lee, Jonathan Denlinger, and Sung-Kwan Mo

Citation: *Appl. Phys. Lett.* **111**, 231603 (2017);

View online: <https://doi.org/10.1063/1.4986425>

View Table of Contents: <http://aip.scitation.org/toc/apl/111/23>

Published by the American Institute of Physics



5 Electronic Measurement Pitfalls to Avoid

Get the whitepaper

Temperature-modulated electronic structure of graphene on SiC: Possible roles of electron-electron interaction and strain

Choongyu Hwang,^{1,a)} Jinwoong Hwang,¹ Ji-Eun Lee,¹ Jonathan Denlinger,² and Sung-Kwan Mo²

¹Department of Physics, Pusan National University, Busan 609-735, South Korea

²Advanced Light Source, Lawrence Berkeley National Laboratory, Berkeley, California 94720, USA

(Received 5 June 2017; accepted 19 November 2017; published online 6 December 2017)

We have investigated the electron band structure of graphene epitaxially grown on an SiC substrate using angle-resolved photoemission spectroscopy. The conical energy spectrum of graphene exhibits a minimum slope at ~ 50 K, which is accompanied by the minimum separation between its two branches. These observations provide a viable route towards the engineering of the electronic properties of graphene using temperature, while the latter suggests a possible evidence of gap engineering via strain induced by the substrate and modulated by temperature. *Published by AIP Publishing.*

<https://doi.org/10.1063/1.4986425>

The search for an efficient way to engineer the electronic properties of a material has been a major issue in applied sciences when a new type of material emerges. Specifically, the presence of two-dimensional (2D) crystals such as graphene makes it possible to realize new approaches engineering their physical properties that barely work in three-dimensional systems.¹ For example, due to dimensionality, the electronic properties of 2D crystals are strongly influenced by dielectric screening² and mechanical strain³ induced by the presence of a substrate.

The Coulombic interaction between charge carriers in graphene exhibits a strong dependence on a dielectric substrate.⁴ In charge neutral graphene, the Fermi velocity, the key factor in determining the electric properties of a material, can be modulated by dielectric screening from a substrate that strongly influences the electron-electron interaction.⁵ The reduced screening leads to the enhanced electron-electron interaction that brings about the deformation of the characteristic linear energy-momentum dispersion of graphene to a logarithmic spectrum, resulting in the increasing Fermi velocity and hence providing a straightforward evidence of non-Fermi liquid behavior of charge neutral graphene.² On the other hand, the Fermi velocity of electron-doped graphene is predicted to decrease with the increasing electron-electron interaction that is well described within the Fermi-liquid theory.^{5,6}

Meanwhile, the plasticity of graphene allows mechanical strain to induce not only the energy gap at the crossing point between the conduction and valence bands, so-called Dirac energy, E_D ,⁷⁻¹² which is one of the ultimate goals for the application of graphene in semiconducting industries, but also pseudomagnetic fields as high as 300 T (Ref. 13) that cannot be achieved using superconducting magnets and electrostatic potentials opening up the way to use graphene as a solar cell.¹⁴ Such a strain has been introduced in graphene by applying strain to a flexible substrate,¹⁵ stretching,¹⁶ or producing local deformation, e. g., by injecting water inbetween graphene and a substrate.¹⁷

The manipulation of the electronic properties of graphene using both the electron-electron interaction and the

mechanical strain can be achieved by varying the temperature of the interface between graphene and a substrate. Graphene shows strong electronic correlations beyond the marginal Fermi liquid self-energy¹⁸ and unusual thermal conductivity violating the Wiedemann-Franz law,¹⁹ hence suggesting a possible formation of strongly coupled Dirac fermionic states. This reveals that temperature is one of the important factors in engineering the electron-electron interaction in graphene. In addition, the negative thermal expansion coefficient of graphene^{20,21} compared to positive ones of most of the substrates²² can cause inevitable mechanical strain^{15,23} that can be controlled by temperature.

In this letter, we report the temperature-dependent angle-resolved photoemission (ARPES) study on graphene epitaxially grown on an SiC substrate. When graphene is intrinsically electron-doped on an SiC substrate,²⁴ the slope of the valence band of the graphene π band and the distance between the two branches of the conical dispersion at the leading edge exhibit a minimum at ~ 50 K. The observed non-monotonic changes of the energy spectrum are attributed to the electron-electron interaction and mechanical strain that are modulated by temperature.

Graphene samples have been prepared by epitaxial growth on an *n*-doped 6H-SiC(0001) crystal.²⁵ An SiC substrate was degassed up to 600 °C for several hours, followed by an annealing process at 900 °C under Si flux for 30 min in a high vacuum chamber with a base pressure of 1×10^{-8} Torr. The sample is further annealed at 1200 °C under Si flux for 5 min to grow single-layer graphene. The overall process leads to the characteristic $6\sqrt{3} \times 6\sqrt{3}$ low-energy-electron diffraction pattern as shown in Fig. 1(a). The graphene sample is transferred to an ultra-high vacuum chamber, followed by another annealing process up to 750 °C to remove air contaminations. The temperature-dependent ARPES experiments have been performed at the beamlines 4.0.3 and 10.0.1.1 of the Advanced Light Source in Lawrence Berkeley National Laboratory using a photon energy of 50 eV. Energy and momentum resolutions at 6 K (170 K) were 16 meV (62 meV) and 0.025 \AA^{-1} (0.032 \AA^{-1}), respectively.

Figure 1(b) shows ARPES intensity maps of graphene on the SiC substrate taken across the K point perpendicular

^{a)}ckhwang@pusan.ac.kr

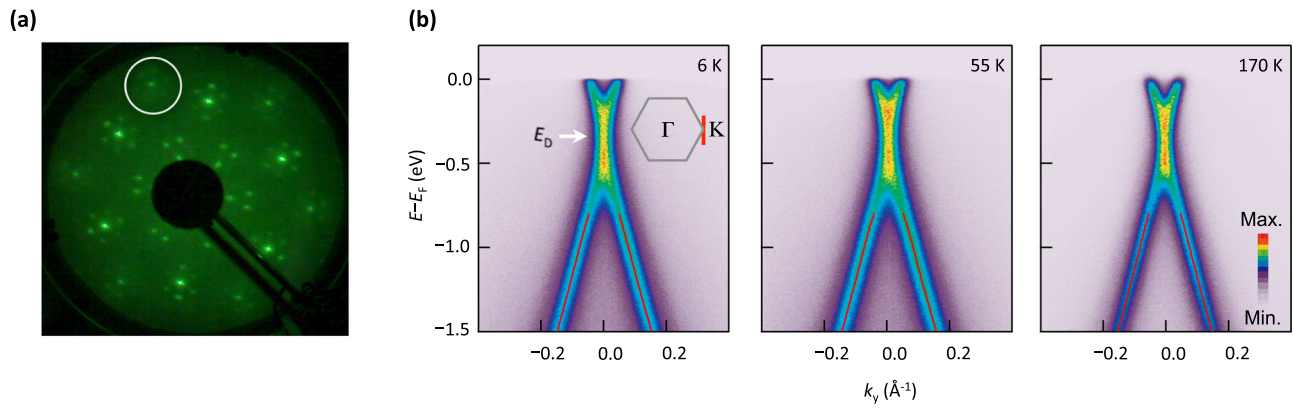


FIG. 1. (a) An LEED image of graphene on an SiC(0001) substrate taken at 98.8 eV. The white circle denotes the graphene 1×1 LEED pattern in addition to the $6\sqrt{3} \times 6\sqrt{3}$ phase corresponding to the graphene/substrate superstructure. (b) ARPES intensity maps of graphene on an SiC(0001) substrate taken perpendicular to the ΓK direction of the graphene unit cell denoted by the red line in the inset at 6 K, 55 K, and 170 K. The white arrow denotes the Dirac energy where conduction and valence bands of graphene meet at a single point. The red lines are Lorentzian fits to the ARPES maps.

to the ΓK direction of the graphene unit cell denoted by the red line in the inset at three different temperatures, 6 K, 55 K, and 170 K. The characteristic conical dispersion is intrinsically electron-doped by the formation of a Schottky barrier at the interface between graphene and the SiC substrate²⁴ so that Fermi energy, E_F , lies ~ 0.4 eV above E_D that is denoted by a white arrow. The origin of the high intensity near E_D is highly controversial²⁶ between the plasmaron that can be influenced by the dielectric screening from the substrate^{4,27} and the in-gap state induced by the substrate.^{28,29} In this study, we focus only on the spectral behavior away from E_D . The red lines shown in each ARPES intensity map are the result of a Lorentzian fit to ~ 160 momentum distribution curves taken by the 3 meV step.

The comparison of the energy-momentum dispersion obtained below E_D provides an unusual temperature dependence of the electron band structure of graphene on SiC, despite the fact that the effect is small. Figure 2(a) shows the energy-momentum dispersion of the graphene π band obtained at 55 K (blue curve) and 170 K (red curve). One can notice that the slope of the dispersion is slightly modified upon changing temperature. The difference in momentum, Δk , shown in the inset indeed denotes that upon approaching towards E_F , the energy-momentum dispersion is gradually separated. This indicates that the slope of the dispersion becomes steeper at higher temperature. To better understand this temperature dependence, Fig. 2(b) shows the slope of the

graphene π band extracted by a line fit to the data from 1.0 eV to 1.5 eV below E_F as a function of temperature. Upon changing temperature, the slope exhibits a non-monotonic change as a function of temperature. The change in the slope of the energy-momentum dispersion holds two possibilities. First, the electron-electron interaction can lead to the change in the slope. When graphene is electron-doped, its charge carrier dynamics is approximately well described by the theory that works for typical metals.⁵ Within the Fermi liquid theory, as the electron-electron interaction becomes stronger, the effective mass becomes heavier so that the slope of the energy-momentum dispersion or velocity of charge carriers decreases. Indeed, in electron-doped graphene, velocity is predicted to decrease with the increasing electron-electron interaction.⁵ Recent thermal conductivity measurements suggest that such an electron-electron interaction in graphene can be modulated by temperature.¹⁹ The thermal conductivity of graphene deviates from the Wiedemann-Franz law due to the enhanced electron-electron interaction with its maximum at ~ 70 K that can further decrease with decreasing impurities such as charge puddles, which is observed from graphene on SiO_2 but not from epitaxial graphene that we have used in our experiments. Within this picture, the maximum thermal conductivity denotes the maximum strength of the electron-electron interaction, suggesting that the observed minimum slope may be attributed to the maximum electron-electron interaction that is modulated by temperature.

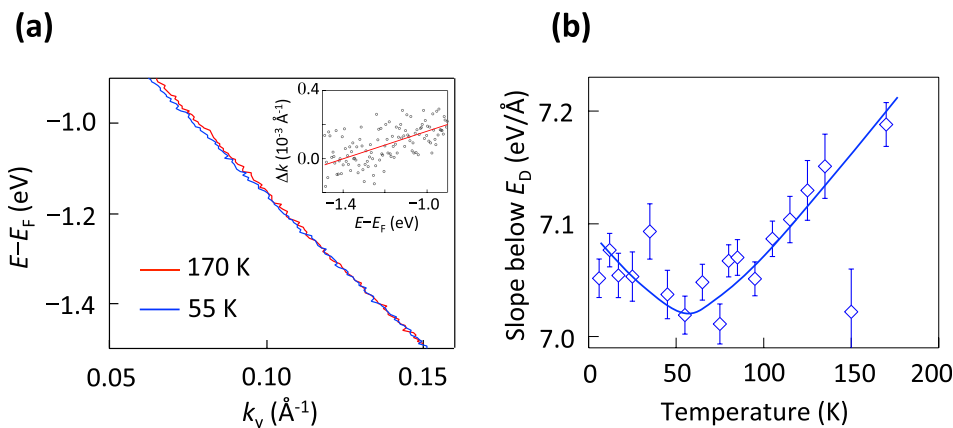


FIG. 2. (a) Fitted energy-momentum dispersion of the energy spectra taken at 55 K (blue curve) and 170 K (red curve). The inset shows the difference of the two dispersions (Δk) as a function of $E - E_F$. (b) The slope of the dispersion obtained by a line fit to the data from 1.0 eV to 1.5 eV below E_F . The blue curve is a guide to the eye.

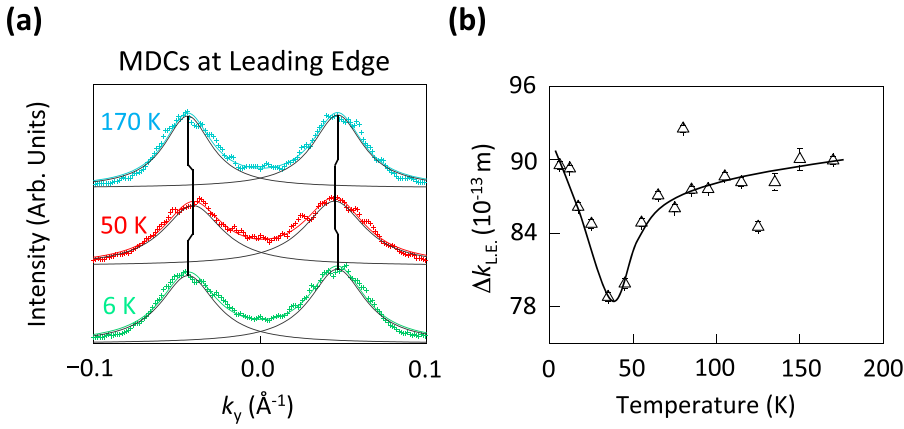


FIG. 3. (a) Momentum distribution curves (MDCs) at the leading edge (L.E.) at three different temperatures, 6 K, 50 K, and 170 K. (b) The distance between the two branches of the conical dispersion at the leading edge ($\Delta k_{L.E.}$) as a function of temperature. The black curve is a guide to the eye.

As an alternative explanation, the competition between thermal expansion and contraction of graphene and the SiC substrate affects the area of the graphene unit cell, respectively, giving rise to the velocity change. Graphene exhibits a negative thermal expansion coefficient of $-8.0 \times 10^{-6} \text{K}^{-1}$,²¹ indicating that the area of the graphene unit cell is expected to change monotonically as a function of temperature when it stands alone. However, it is important to note that the SiC substrate has a positive thermal expansion coefficient of $1.22 \times 10^{-6} \text{K}^{-1}$ at 200 K and $0.27 \times 10^{-6} \text{K}^{-1}$ at 100 K.²² As a result, graphene experiences inevitable mechanical strain by the substrate when temperatures for growth and measurements are different.²³ For this case, the area of the graphene unit cell can change upon changing temperature, resulting in the change in the slope of the energy-momentum dispersion.

The possible change in the area will cause the change in the charge carrier density of graphene, i.e., when the area of the graphene unit cell becomes maximum, the number of charge carriers per unit area will be minimum. In order to investigate this issue, Fig. 3(a) shows momentum distribution curves (MDCs) at three different temperatures, 6 K, 50 K, and 170 K. Throughout the analysis, MDCs at the leading edge (L.E.: the highest kinetic energy of photo-emitted electrons from the occupied states) instead of those at the Fermi wavenumber, k_F , are discussed, due to the ambiguity in determining k_F in the possible presence of charging.³⁰ At 6 K, the separation between the two branches of the conical dispersion of graphene taken at the leading edge, $\Delta k_{L.E.}$, is 0.089 \AA^{-1} , which slightly decreases at 50 K and increases again at 170 K. The temperature-dependent $\Delta k_{L.E.}$ is summarized in Fig. 3(b)

clearly showing minimum $\Delta k_{L.E.}$ at ~ 50 K. The change in $\Delta k_{L.E.}$ directly provides the charge carrier density of graphene by $n \approx (\frac{\Delta k_{L.E.}}{2})^2 \times 3.18 \times 10^{15} \text{ cm}^{-2}$. Thus, minimum $\Delta k_{L.E.}$ at ~ 50 K denotes the minimum charge carrier density, which might be related to the maximum area of the graphene unit cell. However, the maximum area of the graphene unit cell will lead to the maximum slope of the dispersion, which is inconsistent with the result shown in Fig. 2(a). As a result, the observed change in velocity and charge carrier density is not simply understood by the mechanical strain, while above discussion does not exclude the existence of strain applied to graphene by the presence of the substrate.²³

The separation between the two branches of the conical dispersion at constant energy, however, provides another intriguing insight into the strain applied to graphene on an SiC substrate. Figure 4(a) shows the summation of $\Delta k_{L.E.}$ and $\Delta k_{\text{below } 1 \text{ eV}}$, the separation taken at 1.0 eV below the leading edge, as schematically shown in the inset. The $\Delta k_{L.E.} + \Delta k_{\text{below } 1 \text{ eV}}$ versus temperature plot also shows a minimum at 50 K. This safely excludes a charging effect³⁰ as the origin of the temperature dependence of $\Delta k_{L.E.}$ because the trivial charging effect is expected to cause constant $\Delta k_{L.E.} + \Delta k_{\text{below } 1 \text{ eV}}$ for the whole temperature range. Instead, the minimum of $\Delta k_{L.E.} + \Delta k_{\text{below } 1 \text{ eV}}$ may indicate the maximum separation between the conduction and valence bands, which varies as a function of temperature. Although a similar effect can take place by the maximum slope of the dispersion, the slope obtained from 1.0 eV to 1.5 eV below E_F exhibits its minimum within the error bar at 50 K as discussed in Fig. 2(a), excluding this possibility. Given the almost linear

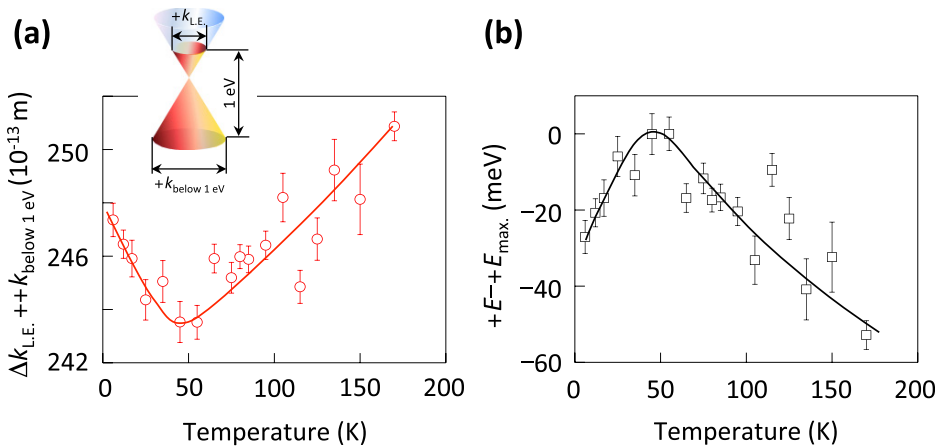


FIG. 4. (a) The summation of $\Delta k_{L.E.}$ and the distance taken at 1.0 eV below the leading edge ($\Delta k_{\text{below } 1 \text{ eV}}$) as a function of temperature. The red curve is a guide to the eye. The inset denotes $\Delta k_{L.E.}$ and $\Delta k_{\text{below } 1 \text{ eV}}$ in the conical band structure. (b) The change in energy gap $\Delta E_{\text{max}} - \Delta E$ as a function of temperature. The black curve is a guide to the eye.

energy-momentum dispersion of graphene near E_D , we attribute the change in $\Delta k_{L.E.} + \Delta k_{below 1 eV}$ to the change in the energy gap around E_D of the graphene π band. Figure 4(b) shows the relative change in the energy gap ΔE with respect to $\Delta E_{max.}$, when ΔE is converted from $\hbar v(\Delta k_{L.E.} + \Delta k_{below 1 eV})$ and $\Delta E_{max.}$ corresponds to the minimum of $\Delta k_{L.E.} + \Delta k_{below 1 eV}$. We find that $\Delta E - \Delta E_{max.}$ shows non-monotonic behavior below and above 50 K, when the black curve is a guide to the eye.

Now, we discuss the unusual non-monotonic change of $\Delta E - \Delta E_{max.}$ as a function of temperature. Epitaxial graphene on SiC experiences mechanical strain by the presence of the substrate.²³ The role of strain in the electronic properties of graphene has been extensively studied by first principles calculations,^{3,7-12,31} e.g., the opening of an energy gap of ~ 100 meV for the uniaxial strain of $\sim 0.2\%$ and ~ 60 meV for $\sim 0.1\%$, resulting in the change in an energy gap of ~ 40 meV.⁷ In graphene on SiC, based on the thermal expansion coefficients of graphene and SiC, the relative difference of the area of graphene and the surface of SiC, i.e., strain, is 0.185% with the decreasing temperature from 200 K to 0 K and 0.085% for the change from 100 K to 0 K.^{21,22} The difference of $\Delta E - \Delta E_{max.}$ between ~ 200 K and 100 K shown in Fig. 4(b) is ~ 35 meV, which is similar to the theoretically predicted value of ~ 40 meV, when we consider that the strain applied to graphene might also be anisotropic due to the anisotropic potential from the substrate.²⁸ Within this picture, the non-monotonic change of $\Delta E - \Delta E_{max.}$ is attributed to the slip of graphene sitting on the substrate with the weak van der Waals force, and the minimum charge carrier density observed in Fig. 3(b) can be understood by the change in the interaction between graphene and the SiC substrate which can modify the Schottky barrier formed in between them.²⁴

In summary, we have investigated the electronic properties of graphene on an SiC substrate. Upon changing temperature, the slope and separation of the conical dispersion of graphene exhibit a minimum at ~ 50 K. While the former can be understood by the temperature-dependent electron-electron interaction in electron-doped graphene, the latter is attributed to strain induced by the different thermal expansion rate of graphene and the SiC substrate. These results suggest a possibility of using graphene in semiconducting devices with controlled quasiparticle dynamics via the interaction with a substrate.

This work was supported by the National Research Foundation of Korea (NRF) grant funded by the Korea government (MSIP) (Nos. 2015R1C1A1A01053065 and 2017K1A3A7A09016384). The Advanced Light Source was

supported by the Office of Basic Energy Sciences of the U.S. Department of Energy under Contract No. DE-AC02-05CH11231.

- ¹A. H. C. Neto and K. Novoselov, *Mater. Express* **1**, 10 (2011).
- ²C. Hwang, D. A. Siegel, S.-K. Mo, W. Regan, A. Ismach, Y. Zhang, A. Zettl, and A. Lanzara, *Sci. Rep.* **2**, 590 (2012).
- ³V. M. Pereira and A. H. Castro Neto, *Phys. Rev. Lett.* **103**, 046801 (2009).
- ⁴A. Bostwick, F. Speck, T. Seyller, K. Horn, M. Polini, R. Asgari, A. H. MacDonald, and E. Rotenberg, *Science* **328**, 999 (2010).
- ⁵S. Das Sarma, E. H. Hwang, and W.-K. Tse, *Phys. Rev. B* **75**, 121406(R) (2007).
- ⁶L. Landau, *JETP* **3**, 920 (1956).
- ⁷Z. H. Ni, T. Yu, Y. H. Lu, Y. Y. Wang, Y. P. Feng, and Z. X. Shen, *ACS Nano* **2**, 2301 (2008).
- ⁸G. Cocco, E. Cadelano, and L. Colombo, *Phys. Rev. B* **81**, 241412(R) (2010).
- ⁹G. Gui, J. Li, and J. Zhong, *Phys. Rev. B* **78**, 075435 (2008).
- ¹⁰V. M. Pereira, A. H. Castro Neto, and N. M. R. Peres, *Phys. Rev. B* **80**, 045401 (2009).
- ¹¹A. B. Preobrajenski, M. L. Ng, A. S. Vinogradov, and N. Maartensson, *Phys. Rev. B* **78**, 073401 (2008).
- ¹²F. Guinea, M. I. Katsnelson, and A. K. Geim, *Nat. Phys.* **6**, 30 (2010).
- ¹³N. Levy, S. A. Burke, K. L. Meaker, M. Panlasigui, A. Zettl, F. Guinea, A. H. Castro Neto, and M. F. Crommie, *Science* **329**, 544 (2010).
- ¹⁴E.-A. Kim and A. H. Castro Neto, *Europhys. Lett.* **84**, 57007 (2008).
- ¹⁵T. Yu, Z. Ni, C. Du, Y. You, Y. Wang, and Z. Shen, *J. Phys. Chem. C* **112**, 12602 (2008).
- ¹⁶W. Bao, F. Miao, Z. Chen, H. Zhang, W. Jang, C. Dames, and C. N. Lau, *Nat. Nanotechnol.* **4**, 562 (2009).
- ¹⁷E. Stolyarova, D. Stolyarov, K. Bolotin, S. Ryu, L. Liu, K. T. Rim, M. Klima, M. Hybertsen, I. Pogorelsky, I. Pavlishin, K. Kusche, J. Hone, P. Kim, H. L. Stormer, V. Yakimenko, and G. Flynn, *Nano Lett.* **9**, 332 (2009).
- ¹⁸H. Ryu, J. Hwang, D. Wang, A. S. Disa, J. Denlinger, Y. Zhang, S.-K. Mo, C. Hwang, and A. Lanzara, *Nano Lett.* **17**, 5914 (2017).
- ¹⁹J. Crossno, J. K. Shi, K. Wang, X. Liu, A. Harzheim, A. Lucas, S. Sachdev, P. Kim, T. Taniguchi, K. Watanabe, T. A. Ohki, and K. C. Fong, *Science* **351**, 1058 (2016).
- ²⁰N. Mounet and N. Marzari, *Phys. Rev. B* **71**, 205214 (2005).
- ²¹D. Yoon, Y.-W. Son, and H. Cheong, *Nano Lett.* **11**, 3227 (2011).
- ²²G. A. Slack and S. F. Bartram, *J. Appl. Phys.* **46**, 89 (1975).
- ²³N. Ferralis, R. Maboudian, and C. Carraro, *Phys. Rev. Lett.* **101**, 156801 (2008).
- ²⁴T. Sellyer, K. V. Emtsev, F. Speck, K.-Y. Gao, and L. Ley, *Appl. Phys. Lett.* **88**, 242103 (2006).
- ²⁵E. Rollings, G.-H. Gweon, S. Y. Zhou, B. S. Mun, J. L. McChesney, B. S. Hussain, A. V. Fedorov, P. N. First, W. A. de Heer, and A. Lanzara, *J. Phys. Chem. Solids* **67**, 2172 (2006).
- ²⁶J. Lischner, D. Vigil-Fowler, and S. G. Louie, *Phys. Rev. Lett.* **110**, 146801 (2013).
- ²⁷A. L. Walter, A. Bostwick, K.-J. Jeon, F. Speck, M. Ostler, T. Seyller, L. Moreschini, Y. J. Chang, M. Polini, R. Asgari, A. H. MacDonald, K. Horn, and E. Rotenberg, *Phys. Rev. B* **84**, 085410 (2011).
- ²⁸S. Kim, J. Ihm, H. J. Choi, and Y.-W. Song, *Phys. Rev. Lett.* **100**, 176802 (2008).
- ²⁹J. Hwang and C. Hwang, *New J. Phys.* **18**, 043005 (2016).
- ³⁰S. D. Lounis, D. A. Siegel, R. Broesler, C. G. Hwang, E. E. Haller, and A. Lanzara, *Appl. Phys. Lett.* **96**, 151913 (2010).
- ³¹S.-M. Choi, S.-H. Jhi, and Y.-W. Son, *Phys. Rev. B* **81**, 081407(R) (2010).